PLATELETS AND THROMBOPOIESIS

Platelet bioreactor-on-a-chip

Jonathan N. Thon,[1,2,3] Linas Mazutis,[3,4,5] Stephen Wu,[1] Joanna L. Sylman,[6] Allen Ehrlicher,[4,7] Kellie R. Machlus,[1,2] Qiang Feng,[8] Shijiang Lu,[8] Robert Lanza,[8] Keith B. Neeves,[6,9] David A. Weitz,[4] and Joseph E. Italiano Jr[1,2,3,10]

[1]Department of Medicine, Brigham and Women's Hospital, Boston, MA; [2]Harvard Medical School, Boston, MA; [3]Platelet BioGenesis, Chestnut Hill, MA; [4]School of Engineering and Applied Sciences, Harvard University, Cambridge, MA; [5]Institute of Biotechnology, Vilnius University, Vilnius, Lithuania; [6]Department of Chemical and Biological Engineering, Colorado School of Mines, Golden, CO; [7]Department of Bioengineering, McGill University, Montreal, Canada; [8]Advanced Cell Technologies, Marlborough, MA; [9]Department of Pediatrics, University of Colorado, Denver, Aurora, CO; and [10]Department of Surgery, Vascular Biology Program, Boston Children's Hospital, Boston, MA

Key Points

- We have developed a biomimetic microfluidic platelet bioreactor that recapitulates bone marrow and blood vessel microenvironments.
- Application of shear stress in this bioreactor triggers physiological proplatelet production, and platelet release.

Platelet transfusions total >2.17 million apheresis-equivalent units per year in the United States and are derived entirely from human donors, despite clinically significant immunogenicity, associated risk of sepsis, and inventory shortages due to high demand and 5-day shelf life. To take advantage of known physiological drivers of thrombopoiesis, we have developed a microfluidic human platelet bioreactor that recapitulates bone marrow stiffness, extracellular matrix composition, micro-channel size, hemodynamic vascular shear stress, and endothelial cell contacts, and it supports high-resolution live-cell microscopy and quantification of platelet production. Physiological shear stresses triggered proplatelet initiation, reproduced ex vivo bone marrow proplatelet production, and generated functional platelets. Modeling human bone marrow composition and hemodynamics in vitro obviates risks associated with platelet procurement and storage to help meet growing transfusion needs. (*Blood*. 2014;124(12):1857-1867)

Introduction

Although platelets (PLTs) play critical roles in hemostasis,[1] angiogenesis,[2] and innate immunity,[3] PLT production remains poorly understood. Consequently, PLT units are derived entirely from human donors, despite serious clinical concerns owing to their immunogenicity and associated risk of sepsis.[4] More than 2.17 million apheresis-equivalent PLT units are transfused yearly in the United States[5,6] at a cost of >$1 billion per year. Although demand for PLT transfusions has increased markedly in the past decade, a near-static pool of donors and a 5-day PLT unit shelf life resulting from bacterial contamination[7] and storage-related PLT deterioration,[8] have resulted in significant PLT shortages.[9] Furthermore, artificial platelet substitutes have failed to replace physiological platelet products.[10] An efficient, donor-independent PLT bioreactor capable of generating clinically significant numbers of functional human PLTs is necessary to obviate risks associated with PLT procurement and storage, and help meet growing transfusion needs.

In vivo, megakaryocytes (MKs) PLT progenitors sit outside blood vessels in the bone marrow (BM) and extend long, branching cellular structures designated proPLTs into the circulation from which PLTs are released.[11-15] Nearly 100% of human adult MKs must produce $\sim 10^3$ PLTs each to account for circulating PLT counts.[16] Although functional human PLTs were first grown in vitro in 1995,[17] to date only ~10% of human MKs initiate proPLT production in culture. This results in yields of 10^{1-2} PLTs per $CD34^+$ cord blood-derived or embryonic stem cell-derived MK,[18] which are themselves of limited availability, constituting a significant bottleneck in the ex vivo production of a PLT transfusion unit. Although second-generation cell culture approaches have provided further insight into the physiological drivers of PLT release, they have been unable to recreate the entire BM microenvironment, exhibiting limited individual control of extracellular matrix (ECM) composition,[19,20] BM stiffness,[21] endothelial cell contacts,[22,23] and vascular shear stresses,[24,25] and have been unsuccessful in synchronizing proPLT production, resulting in nonuniform PLT release over a period of 6 to 8 days.[26] Moreover, the inability to reproduce the BM microenvironment ex vivo, and resolve physiological proPLT extension and release by high-resolution live-cell microscopy, has significantly hampered efforts to study the cytoskeletal and signaling mechanics of PLT production. Biomimetic platforms that model human BM are needed to support drug development and establish new treatments for thrombocytopenia.

This article describes the development of a scalable, third-generation, human-induced pluripotent stem cell-derived MK-compatible PLT bioreactor that uses biologically inspired engineering to fully integrate the major chemical and physical components of the BM stroma under high-resolution live-cell microscopy. This work

Submitted May 9, 2014; accepted July 8, 2014. Prepublished online as *Blood* First Edition paper, July 21, 2014; DOI 10.1182/blood-2014-05-574913.

The online version of this article contains a data supplement.

There is an Inside *Blood* Commentary on this article in this issue.

The publication costs of this article were defrayed in part by page charge payment. Therefore, and solely to indicate this fact, this article is hereby marked "advertisement" in accordance with 18 USC section 1734.

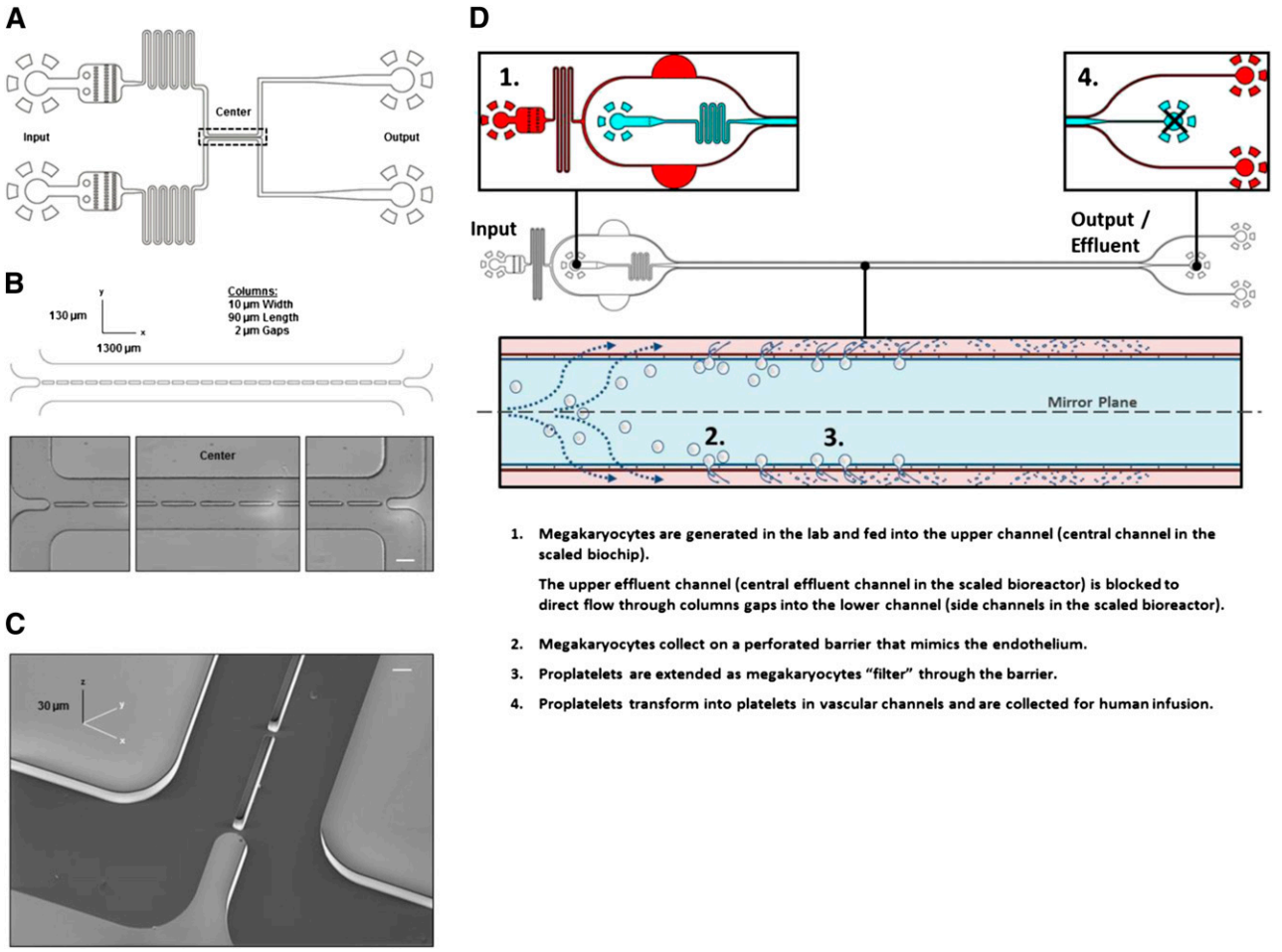

Figure 1. PLT bioreactor design. (A) PLT bioreactors are based on custom-built polydimethylsiloxane (silicon-based organic polymer) bonded to glass slides, and are comprised of an upper and lower microfluidic channel separated by a series of columns. (B) The 2 μm gaps separate columns to trap MKs entering the upper channel from crossing into the lower channel upon fluid withdrawal from the outlet of the lower channel. (C) Scanning electron micrograph of bioreactor central channels. (D) Scaled bioreactor design showing typical device operation. Scale bars represent 50 μm (B) and 5 μm (C).

constitutes a major advance in PLT biology by providing a window into the complex physiology of thrombopoiesis, and a biomimetic platform to elaborate the physiological drivers of proPLT production, accelerate PLT release, and generate a donor-independent source of functional human PLTs for infusion.

Methods

Microfluidic bioreactor design and fabrication

To ensure efficient gas exchange and support high-resolution live-cell microscopy during cell culture, microfluidic bioreactors were constructed from transparent polydimethylsiloxane (PDM), which is a cell-inert silicon-based organic polymer[27] bonded to glass slides. The microfluidic bioreactor consists of 2 inlet channels containing passive filters used to trap air bubbles and dust, followed by fluid resistors used to dampen fluctuations in flow rate arising during chip operation. The inlet channels meet in a central channel 1300 μm long and 130 μm wide, separated by a series of columns (10 μm wide and 90 μm long) spaced 2 μm apart. For the purposes of clarity the "upper channel" should be construed to represent the top-most channel in the original bioreactor (Figure 1A-C) and the central channel in the scaled bioreactor (Figure 1D). Likewise, the "lower channel" should be construed to represent the bottom-most channel in the original bioreactor (Figure 1A-C) and the side channels in the scaled bioreactor (Figure 1D). Primary MKs become trapped in these gaps while moving from the upper channel into the lower channel. Two outlet channels collect the effluent.

Rectangular microfluidic channels 30 μm deep for mouse fetal liver culture-derived–MKs and 10 μm deep for human-induced pluripotent stem cell culture (hiPSC)-MKs were fabricated using soft lithography as previously described.[28] AutoDesk software in AutoCAD was used to design the desired two-dimensional pattern and printed on a photolithography chrome mask. The silicon wafer (University Wafers, Boston, MA) was spin coated with SU-8 3025 photoresist (Michrochem, Newton, MA) to a 30 μm film thickness (Laurell Technologies, North Wales, PA), baked at 65°C for 1 minute and 95°C for 5 minutes, and exposed to UV light (~10 mJ · cm^2) through the chrome mask for 30 seconds. The unbound SU-8 photoresist was removed by submerging the substrate into propylene glycol monomethyl ether acetate for 7 minutes. PDMS was poured onto the patterned side of the silicon wafer, degassed, and cross-linked at 65°C for ~12 hours. After curing, the PDMS layer was peeled off the mold and the inlet/outlet holes were punched with a 0.75 mm diameter biopsy punch. The microchannels were sealed by bonding the PDMS slab to a glass coverslide (#1.5, 0.17 × 22 × 50 mm; Dow Corning, Seneffe, Belgium) after treatment with oxygen plasma (PlasmaPrep 2; GaLa Instrumente GmbH, Bad Schwalbach, Germany). Samples were infused into the microfluidic bioreactor via polyethylene/2 tubing (Scientific Commodities, Lake Havasu City, AZ) using 1 mL syringes equipped with 27-gauge needles (Beckton Dickinson, Franklin Lakes, NJ). Flow rates of liquids were controlled by syringe pumps (PHD 2000; Harvard Apparatus, Holliston, MA).

Microfluidic bioreactor operation

Bioreactors were coated with a 0.22 μm filtered (Millipore, Billerica, MA) 10% bovine serum albumin solution for 30 minutes to prevent direct cell contact with glass. Primary MKs and media were infused in the top-left and bottom-left inlets, respectively, at a rate of 12.5 μL/hour using a two-syringe microfluidic pump (Harvard Apparatus, Holliston, MA). When the top-right outlet is closed, both input solutions are redirected out the bottom-right outlet causing primary MKs to trap in the gaps separating the 2 middle channels.

Results

PLT bioreactor models the physiological characteristics of human BM

PLT bioreactors were designed to recapitulate the dimensions of human venules[29] in the BM (Figure 1A) and are comprised of upper and lower microfluidic channels separated by a series of columns (spaced 2 μm apart) (Figure 1B-C) to model proPLT extension through gaps in vascular endothelium under controlled flow conditions. To scale PLT production the bioreactor was lengthened, and upper and lower microfluidic channels were mirrored as outlined in Figure 1D. Precise bioreactor dimensions are outlined in the supplemental Material (available on the *Blood* Web site).

Our bioreactor was designed to support integration of microchannel size, ECM composition, BM stiffness, endothelial cell contact, and hemodynamic vascular shear stress within a single platform device. The upper and lower channels can be selectively coated with ECM proteins to reproduce the biochemical composition of the BM and blood vessel microenvironments (Figure 2A). By blocking the upper right channel output to direct flow across the bioreactor, primary mouse MKs infused along the top channel become sequentially trapped between the columns and extend proPLTs into the lower channel (Figure 2B), recapitulating physiological proPLT extension (white arrow).[11,30-32] To model three-dimensional ECM organization and physiological BM stiffness (250 Pa)[33](supplemental Figure 1A-D), primary mouse MKs were infused in a 1% alginate or 3 mg/mL growth factor reduced Matrigel solution. Alginates are naturally derived polysaccharides that are cell-inert and can be modified with RGD-containing cell adhesion ligands to specifically reproduce MK-matrix interactions in the BM, such as glycoprotein (GP)IIb/IIIa receptor binding to fibrinogen.[34] Matrigel is a solubilized basement membrane preparation that is comprised primarily of laminin and collagen type IV, which are both known agonists of proPLT production, and is preferred over collagen type I-based hydrogels, which is a known inhibitor of proPLT production.[19,20] Hydrogels were polymerized within the microfluidic bioreactor, selectively embedding the MKs in a three-dimensional gel within the upper channel, while retaining vascular flow in the lower channel (0.02 μm fluorescent bead streaking, fluorescein isothiocyanate-dextran fluorescence) (supplemental Figure 1C). MK distance from the lower channel could be tightly controlled by regulating infusion rate and starting/stopping flow on the microfluidic pump (supplemental Figure 1A-B). Alginate did not inhibit proPLT production (supplemental Figure 1E). To further reproduce BM blood vessel physiology, human umbilical vein endothelial cells (HUVECs) were selectively seeded on fibronectin in the lower channel and grown to confluency (Figure 2C). HUVECs were positive for CD31 (biomarker) and DAF-2 DA (nitric oxide, data not shown). MK trapping, BM stiffness, ECM composition, microchannel size, hemodynamic vascular shear stress, and endothelial cell contacts can be combined to reproduce the BM vascular niche in vitro, as is represented with primary mouse MKs in Figure 2D.

In the BM, MKs extend proPLTs into sinusoidal blood vessels 20 to 60 μm in diameter (comparable in size to small arterioles) where they are thought to experience low wall shear rates of ~100 seconds^{-1}.[35-37] To reproduce vascular shear stress of BM sinusoids, MKs were infused in the upper channel of the scaled microfluidic bioreactor and flow was directed across the scaled PLT bioreactor. MK behavior was monitored by ×10 to ×150 magnification high-resolution live-cell microscopy and released PLTs were collected from the effluent. Shear rates were characterized by computational fluid dynamics within the central region of the scaled microfluidic bioreactor (Figure 2E) and were tightly controlled using 2 syringe pumps (1 for each channel). Shear rates within the bioreactor were linearly proportional to infusion rates and were adjusted to span well below and above the physiological range (Figure 2F) (100-2500 seconds^{-1}).[38] Peaks in this figure represent sequential gap junctions through which shear is highest. MKs infused in the upper channel occupy each gap sequentially, beginning with the furthest gap (position closest to the output channel) and moving inward toward the inlet channel. Local shear stress was determined by multiplying the shear rate by the media viscosity at 37°C (1.2 mPa · seconds, which is equivalent to human plasma). Although shear rates at empty gaps increased with distance from the inlet channel, on MK trapping flow is redirected through the next available gap, such that individual MKs continued to experience physiological (912-936 mPa) shear stresses at their site of trapping. This effect is independent of number of blocked sites and approximately one-third of gaps remained open throughout the course of the experiment (Figure 2G and supplemental Figure 2).

Vascular shear stress triggers proPLT production, physiological extension, and release

In vivo, BM MKs extend proPLTs in the direction of blood flow and release PLTs, proPLTs, large cytoplasmic fragments (prePLTs), and even whole MKs into sinusoidal blood vessels.[15] These cells may become trapped in the pulmonary microvascular bed,[16,39] and are believed to mature in the circulation.[40] To determine the effect of physiological shear stress on PLT production, mouse fetal liver culture-derived MKs (hereafter described as "primary mouse MKs") were isolated on culture day 4 and characterized by size and ploidy before being infused into the bioreactor (Figure 3A-B). One of the major challenges in producing transfusable PLTs in vitro has been identifying factors that trigger proPLT production. Under static conditions, primary mouse MKs begin producing proPLTs ~6 hours postisolation and reach maximal proPLT production at 18 hours (Figure 3B).[26] By comparison, primary mouse MKs under physiological shear stress (~600 mPa) began producing proPLTs within seconds of trapping, reaching maximal proPLT production and bioreactor saturation within the first 2 hours of culture (Figure 3C). Primary mouse MKs cultured under physiological shear stress produced fewer, longer proPLTs that were less highly branched relative to static cultures (supplemental Movies 1-2). ProPLTs in shear cultures were uniformly extended into the lower channel and aligned in the direction of flow against the vascular channel wall, recapitulating physiological proPLT production[11,30,32] (supplemental Movie 2). The percent of proPLT-producing primary mouse MKs under physiological shear stress were doubled over static cultures[26] to ~90% (Figure 3D).

ProPLTs are the assembly lines of PLT production, and another major challenge in generating clinical numbers of PLTs for infusion

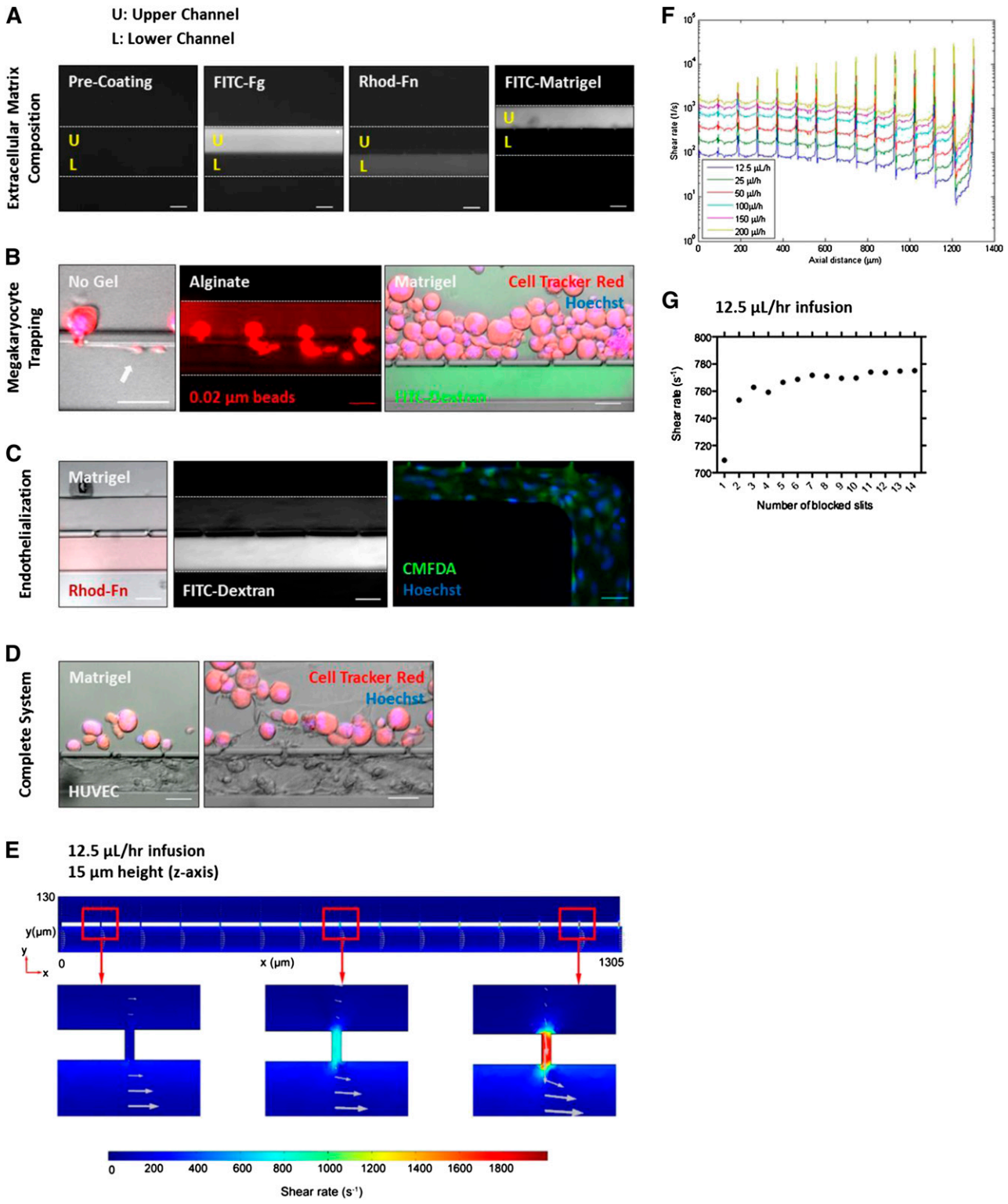

Figure 2. PLT bioreactor models major components of BM. Primary mouse MKs are shown. (A) The upper and lower channels can be selectively coated with ECM proteins to reproduce osteoblastic and vascular niche composition. (B) MKs trap at gaps and extend proPLTs into the lower channel (white arrow). MKs can be selectively embedded in alginate or Matrigel gels, modeling three-dimensional ECM organization and physiological BM stiffness (250 Pa). Vascular flow is retained in the lower channel as demonstrated by 0.02 μm fluorescent bead streaking and fluorescein isothiocyanate-dextran fluorescence. (C) HUVECs can be selectively cultured in ECM-coated channels to reproduce blood vessel physiology. (D) MK trapping, BM stiffness, ECM composition, micro-channel size, hemodynamic vascular shear stress, and endothelial cell contacts can be combined to reproduce human BM in vitro. (E) Shear rate distribution along the length of the channel. Arrows indicate the magnitude and direction of the velocity field. (F) Fluid shear rates are well-characterized and can be tightly regulated across the bioreactor as a function of flow rate. (G) Regardless of the number of occupied slits, trapped MKs experience physiological shear stresses at gap junctions. Media viscosity is 1.20 mPa · s. Scale bars represent 50 μm (A-D).

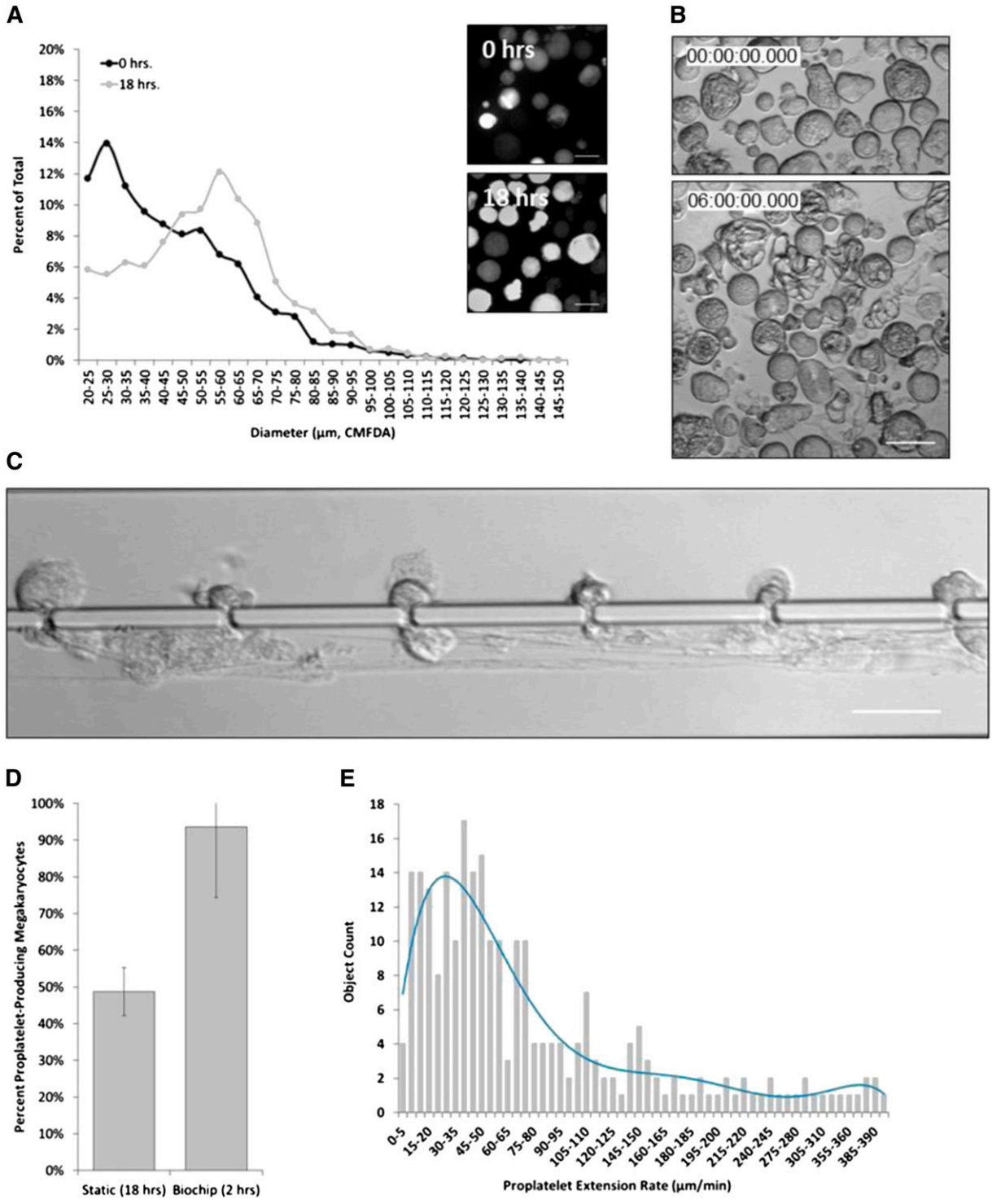

Figure 3. Physiological shear stress induces proPLT production in primary mouse MKs. (A) Primary mouse MKs range between 20 and 85 μm in diameter on culture day 4, and become larger (40-100 μm) if they do not form proPLTs. (B) MKs in static culture begin producing proPLTs at 6 hours postpurification and reach maximal proPLT production at 18 hours. (C) Primary mouse MKs under physiological shear stress (~600 mPa) begin producing proPLTs immediately upon trapping and extend/release proPLTs within the first 2 hours of culture. (D) Percent proPLT-producing primary mouse MKs under physiological shear stress are increased significantly to ~90% over static cultures (~50%).[26] (E) ProPLT extension rates under physiological shear stress are increased significantly (to ~30 μm/min) over static cultures (0.85 μm/min).[41] Scale bars represent 50 μm (A-C).

has been that in vitro cultures extend proPLTs at a significantly slower rate than what has been observed in vivo. Application of physiological shear stress in our microfluidic bioreactor increased the proPLT extension rate by an order of magnitude above static culture controls[41] (supplemental Figure 6I) to ~30 μm/min (Figure 3E), which agree with physiological estimates of proPLT extension rates from intravital microscopy studies in living mice[11] and support increased PLT production in vitro.

Early histologic studies in both humans and mice have predicted that whole MKs, as well as MK fragments may be squeezing through

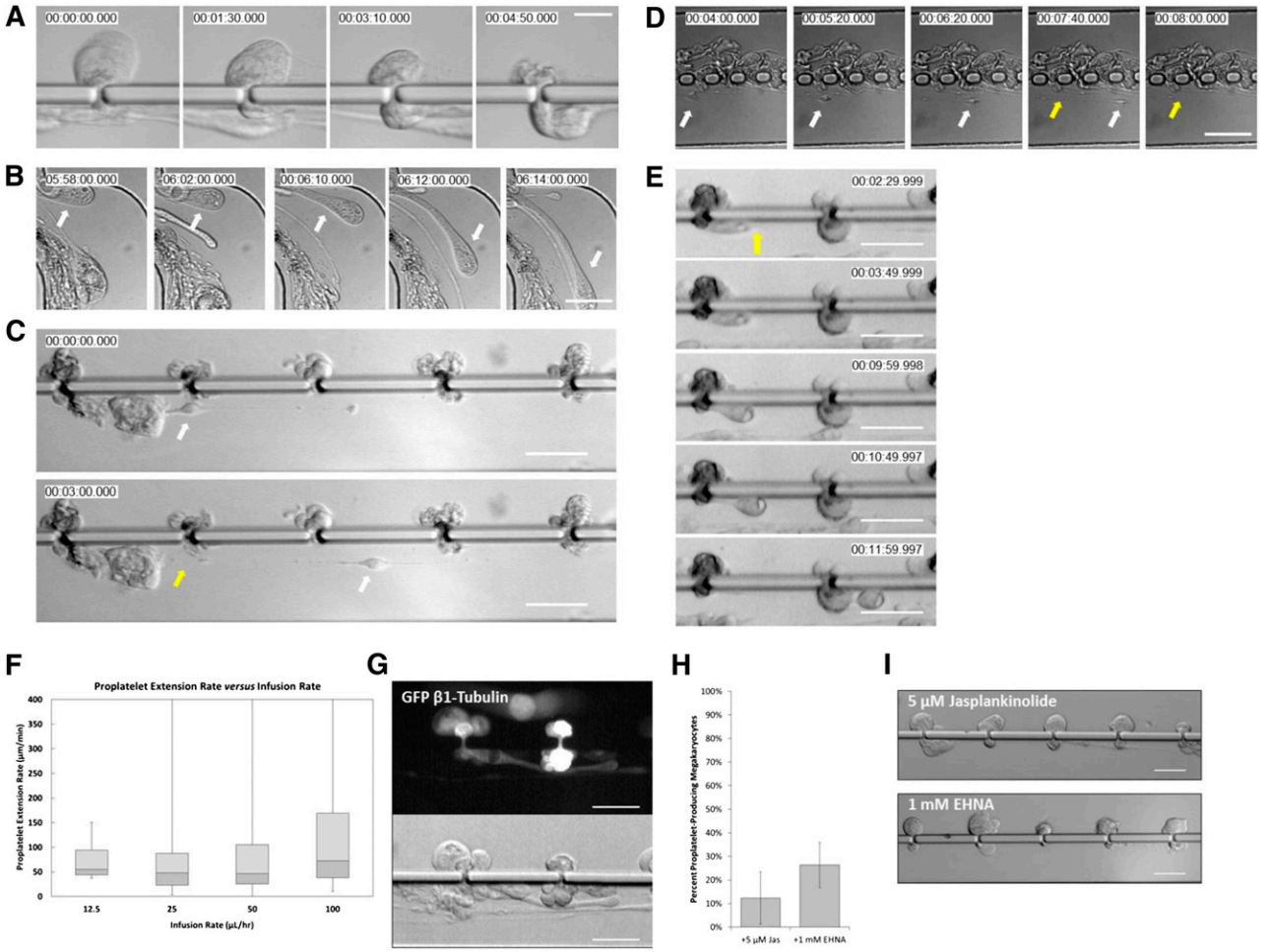

Figure 4. Shear stress-mediated proPLT extension is a cytoskeleton-driven process. (A) Approximately 100 μm diameter primary mouse MK squeezing through 2 μm gap. (B) Release of large MK fragment from primary mouse MK into the lower channel resulting in prePLT formation. White arrows indicate proPLT extension. (C) ProPLT extension rates vary at different positions along the shaft, predictive of a regulated cytoskeletal driven process. The hiPSC-derived MKs are shown. White arrows indicate proPLT extension, and yellow arrows indicate site of abscission event. (D) Individual release events (yellow arrow) are routinely captured by high-resolution live-cell microscopy at different positions along the proPLT shaft. White arrow denotes proPLT end. Primary mouse MKs are shown in an earlier bioreactor design in which gaps are spaced 45 μm apart. (E) PrePLTs form at new proPLT ends after each abscission event (yellow arrow). Primary mouse MKs are shown. (F) Increasing shear stress from 100 to 1000 seconds^{-1} does not increase proPLT extension rate in primary mouse MKs. Data are represented as a box-and-whisker plot where light gray indicates the upper quartile and dark gray indicates the lower quartile. (G) Primary mouse MKs retrovirally transduced to express GFP-β1 tubulin show proPLT extensions are comprised of peripheral MTs that form coils at the PLT-sized ends. (H) Jasplakinolide, 5 μM ([Jas], actin stabilizer) and 1 mM erythro-9-(3-[2-hydroxynonyl]) ([EHNA], cytoplasmic dynein inhibitor) inhibit shear-induced proPLT production in primary mouse MKs. (I) Representative images of drug-induced inhibition of proPLT production under physiological shear stress (from H). Scale bars represent 50 μm.

gaps or fenestrations in the vascular endothelium lining BM blood vessels to trap in the pulmonary circulatory bed.[16,39] Large PLT intermediates called prePLTs were recently discovered in blood,[40] and venous infusion of mouse BM-derived MKs, fetal liver culture–derived MKs,[42] and prePLTs[25] into mice produced PLTs in vivo. In the present study, ≥100 μm diameter primary mouse MKs were routinely observed squeezing through 2 μm gaps (Figure 4A and supplemental Movie 3A-B) or extending large MK fragments (Figure 4B and supplemental Movie 4), supporting a model of vascular PLT production. Although rarely observed under static conditions, abscission events were routinely captured by high-resolution live-cell microscopy and occurred at variable positions along the proPLT shaft, releasing both prePLT-sized intermediates (3-10 μm diameter) (supplemental Movie 5) and PLTs (1.5-3 μm diameter) (Figure 4C). Figure 4D and supplemental Movie 6 represent an earlier bioreactor design in which gaps are spaced 45 μm apart. After each abscission (yellow arrow), the resulting proPLT end formed a new prePLT-sized swelling at the tip, which was subsequently extended and released, repeating the cycle (Figure 4E and supplemental Movie 7).

Although shear stress was kept constant, proPLT extension rates varied at different positions along the shaft, predictive of a regulated cytoskeletal driven mechanism of proPLT elongation. Although these studies were performed with primary mouse MKs, this was also true of hiPSC-MKs (Figure 4C, hiPSC-MK culture shown). Increasing shear stress within the physiological range did not affect the median proPLT extension rate or the distribution of proPLT extension rates in primary MK culture (Figure 4F), and proPLT projections in primary mouse MKs retrovirally transduced to express green flourescent protein-β1 tubulin were comprised of peripheral MTs that formed coils at the PLT-sized ends (Figure 4G and supplemental Movie 8). ProPLTs reached lengths exceeding 5 mm (supplemental Figure 4A) and resisted shear stress up to 1200 mPa in vitro; recapitulating physiological examples of proPLT production from intravital microscopy[11] and demonstrating that abscission events were not caused by membrane tethering. To confirm that

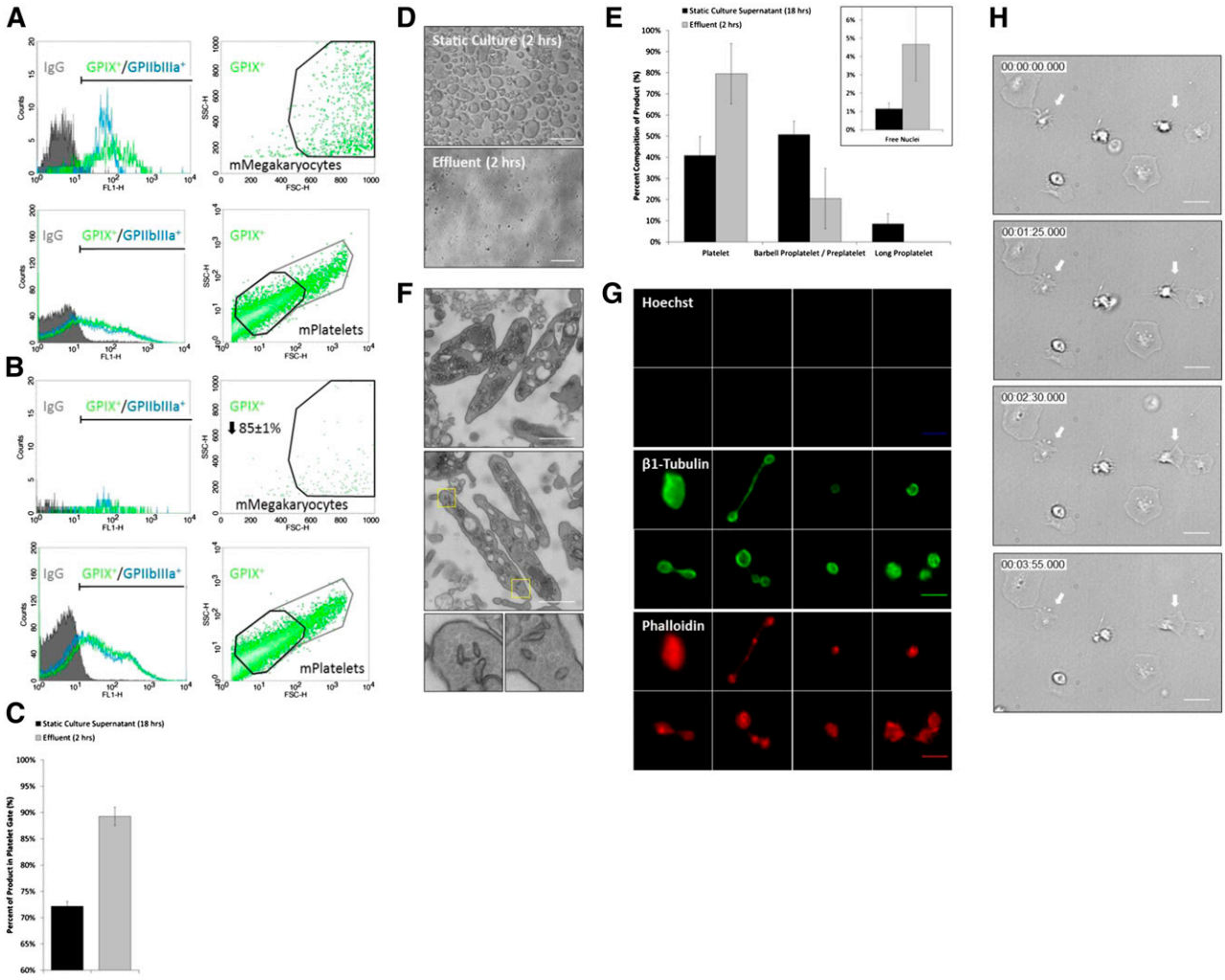

Figure 5. Bioreactor-derived mPLTs manifest structural and functional properties of mouse blood PLTs. (A) Biomarker expression, and forward/side scatter and relative concentration of GPIX$^+$ primary mouse MKs infused into bioreactor after isolation on culture day 4, and (B) effluent collected from bioreactor 2 hours postinfusion. (C) Application of shear stress shifts GPIX$^+$ product toward more PLT-sized cells relative to static culture supernatant. (D) Comparison of primary mouse MK culture product under static and bioreactor conditions over a period of 2 hours. (E) Application of shear stress shifts product toward more PLT-sized β1-tubulin$^+$ Hoechst$^-$ cells (labeled Platelet) relative to static culture supernatant. Insert shows quantitation of free nuclei in effluent. (F) Bioreactor-mPLTs are ultrastructurally similar to mouse blood PLTs and contain a cortical MT coil, open canalicular system, dense tubular system, mitochondria, and characteristic secretory granules. Bottom inserts show magnification of yellow boxes at PLT ends. (G) Bioreactor-mPLTs and PLT intermediates are morphologically similar to mouse blood PLTs (supplemental Figure 6) and display comparable MT and actin expression. Top 8 panels show Hoechst labeling, middle 8 panels show β1-Tubulin labeling bottom 8 panels show Phalloidis labeling. (H) Bioreactor-mPLTs form filopodia/lamellipodia on activation and spread on glass surface. Scale bars represent 5 μm (D,G-H) and 1 μm (F).

shear stress-induced proPLT extension was cytoskeletal-driven, primary mouse MKs were incubated with 5 μM Jasplakinolide ([Jas] actin stabilizer) or 1 mM *erythro*-9-(3-[2-hydroxynonyl]) (EHNA, cytoplasmic dynein inhibitor) prior to infusion into the microfluidic bioreactor. Inhibition of cytoskeletal reorganization significantly reduced shear stress-induced proPLT production from 90% to 12% (Jas) and 26% (EHNA), respectively (Figure 4H-I and supplemental Movies 9-10), and inhibited proPLT extension under static culture conditions (supplemental Figure 4B). These studies validate the use of our PLT bioreactor as a platform technology to study physiological proPLT production under vascular shear stress.

Bioreactor-derived PLTs manifest structural and functional properties of blood PLTs

To establish PLT yield, biomarker expression, forward/side scatter, and relative concentration of GP IX$^+$ primary mouse MKs were measured by flow cytometry immediately before infusion into the bioreactor on culture day 4 (Figure 5A). Effluent was collected from the bioreactor 2 hours postinfusion and compared with primary mouse MK input (Figure 5B). Input MKs and effluent PLTs both expressed GP IX and IIbIIIa on their surface and displayed characteristic forward/side scatter. The application of shear stress shifted the cellular composition of the effluent toward more PLT-sized GP IX$^+$ cells relative to static culture supernatant isolated on culture day 5 (Figure 5C). There were 85 ± 1% of primary mouse MKs converted into PLTs over 2 hours, which agreed with our quantitation of percent proPLT production (Figure 3D) and constitutes a significant improvement over static cultures (Figure 5D). Continuous media perfusion at ~500 seconds^{-1} over 2 hours in our microfluidic bioreactor yielded an additional 24 ± 7 PLTs per MK over static primary mouse MK culture PLT yields (18 PLTs/MK) (supplemental Figure 3C); this improvement more than doubled PLT production rates over static cultures and resulted in a total PLT yield of ~42 PLTs per MK from $5.7 \times 10^4 \pm 3.4 \times 10^4$ MKs per mL. This constitutes a major advance in PLT production rate over existing culture approaches that generate comparable PLT numbers over a longer period of time (6-8 days).[43,44]

To quantify the morphologic composition of our product, the bioreactor effluent was probed for β1 tubulin (PLT-specific tubulin isoform) and Hoechst (nuclear dye), and analyzed by immunofluorescence microscopy (supplemental Figure 5A). Cells were binned according to their morphology and size (Figure S5B), and compared with static primary mouse MK culture supernatants. The application of shear stress shifted the cellular composition of the effluent toward more PLT-sized β1 tubulin$^+$ Hoechst$^-$ cells (Figure 5E), which agreed with flow cytometry data (Figure 5C) and resulted in a product that was more similar in composition to the distribution of PLT intermediates in whole blood.[40] Quantitation of free nuclei in the effluent (Figure 5E, insert) confirmed increased bioreactor-mediated PLT production vs static culture and established PLT yields of ~20 ± 12 PLTs per MK above static culture yields, which agree with flow cytometry data.

Bioreactor PLTs were ultrastructurally indistinguishable from mouse blood PLTs by electron microscopy and contained a cortical MT coil, open canalicular system, dense tubular system, mitochondria, and α- and dense-granules (Figure 5F). Bioreactor-PLTs and PLT intermediates displayed comparable MT and actin organization to mouse blood PLTs by immunofluorescence microscopy (Figure 5G) and spread normally on contact activation with glass, forming both filpodia and lamellipodia (Figure 5H and supplemental Movie 11).

Application of bioreactor to human PLT production

Can PLT production be recapitulated with human MKs? To generate human PLTs, primary mouse MKs in our bioreactor were replaced with hiPSC-derived MKs, which (unlike CD34$^+$ human cord blood-derived MKs or embryonic stem cell-derived MKs) provide a virtually unlimited source of MKs for infusion. The hiPSC-MKs were isolated on culture day 15, once they had reached maximal diameter (20-60 μm) (Figure 6A) and were ultrastructurally similar to primary human MKs (Figure 6B). The detailed generation and characterization of these hiPSC-MKs is outlined in another manuscript (Q.F., N. Shabrani, J.N.T., H. Huo, A. Thiel, K.R.M., K. Kim, J. Brooks, F. Li, C. Luo, E.A. Kimbrel, J. Wang, K.-S. Kim, J.E.I., J. Cho, S.-J. Lu, and R.L., manuscript submitted 2014). In static culture, our hiPSC-MKs began producing proPLTs at 6 hours postisolation and reached maximal proPLT production at 18 hours (Figure 6C). By comparison, hiPSC-MKs under physiological shear stress (~600 mPa) began producing proPLTs immediately upon trapping and extended/released proPLTs within the first 2 hours of culture (Figure 6D and supplemental Movies 12-14). Percent of proPLT-producing hiPSC-MKs under shear stress were increased significantly (~90% of total MKs) over static cultures (~10%) (Figure 6E). ProPLT extension rates were slightly lower than primary mouse MKs (~19 μm/min vs 30 μm/min) (Figure 6F) and more closely approximated physiological controls[11] (supplemental Figure 6I). The hiPSC-MK proPLT production and PLT release was otherwise morphologically identical to primary mouse MKs. The hiPSC-MK-derived bioreactor-PLTs displayed forward and side scatter, and surface biomarker expression characteristic of human blood PLTs (Figure 6G). Bioreactor PLTs were ultrastructurally indistinguishable from human blood PLTs by electron microscopy[45] (Figure 6H), which were anucleate and displayed comparable morphology and MT expression to human blood PLTs by immunofluorescence microscopy (Figure 6I), and spread normally upon contact activation with glass, forming both filpodia and lamellipodia (Figure 6J). Continuous media perfusion at ~500 seconds^{-1} over 2 hours in our microfluidic bioreactor yielded a total of ~30 PLTs per MK from $1.9 \times 10^4 \pm 1.3 \times 10^4$ MKs per mL (supplemental Figure 3D). Taken together, these data demonstrate that hiPSC-MKs can be applied to our biomimetic microfluidic bioreactor to model physiological human PLT production and generate potentially unlimited numbers of functional human PLTs for infusion. Representative data for mouse and human platelet controls are included in supplemental Figure 6.

Discussion

This study capitalizes on a novel microfluidic design to recapitulate human BM and blood vessel physiology ex vivo, and to dramatically and significantly improve the rate of platelet production over static cultures, thereby paving the way for additional improvements in platelet yield with the ultimate goal of generating a donor-independent source of functional human platelets for infusion. Two major quantitative roadblocks persist in the development of donor-independent PLTs for therapeutic use: (1) generating sufficient numbers (~3×10^8) of human MKs to support the production of 1 PLT transfusion unit (~3×10^{11} PLTs); and (2) generating physiological numbers of functional human PLTs (~10^3) per MK.[18] The development of human embryonic stem cell cultures (hESC),[44,46] and more recently, hiPSC[47] (Feng Q et al, manuscript submitted 2014) offer a physiologically relevant and potentially unlimited source of progenitor cells that can be differentiated into human MKs in vitro to address the first quantitative roadblock.[48] Indeed, because PLTs are anucleate, PLT bioreactor-derived units could be irradiated prior to infusion, addressing concerns that cellular products derived from hESC or hiPSCs could be oncogenic or teratogenic.[49]

Nevertheless, attempts to study the environmental drivers of PLT production have fallen short. A major limitation of two-dimensional liquid cultures has been their inability to account for three-dimensional BM composition and stiffness, directionality of proPLT extension, and proximity to venous endothelium.[15,24,25] Alternatively, intravital microscopy studies have provided physiologically accurate examples of proPLT production, however, poor resolution and limited control of the microenvironment has prohibited detailed study of how the BM microenvironment contributes to PLT release.[11,15] Nakagawa et al[50] recently published 3 bioreactor designs to produce human PLTs at scale from hiPSC- and ESC-derived MKs. Although all 3 designs intend to use flow to trigger PLT production, direct visualization of proPLT production is severely restricted, shear rates are not modeled, and the profile of flow within the devices is unknown. Although there are superficial similarities to our bioreactor, there are major limitations to all 3 of Nakagawa et al's[50] bioreactor designs that are worth noting. Bioreactor design 1 traps MKs against HUVECs within 23 μm diameter porous channels. Although the authors do not show evidence of the HUVECs within the bioreactor, and it is unclear whether HUVECs are confluent, viable, or necessary for proPLT production in their bioreactor system, HUVECs are undesirable in a PLT product and may constitute a significant transfusion risk. PLT purity and yield from this device is not reported. Bioreactor design 2 reduces pore size to 8 μm and removes HUVEC coculture, but achieves marginal (<1.5-fold) improvements in PLT yield over static culture for 2 hESC-MKs replicates. Bioreactor design 3 decreases pore size further to 4 μm and infuses MKs at a 60° angle to lateral flow. Nakagawa et al[50] reports 71 755 PLTs from 120 000 hESC-MKs, constituting a total PLT yield of 0.59 PLTs per MK. The hiPSC-MK PLT yields are not reported. Neither bioreactor supports visualization of live PLT production at high resolution in real-time to resolve the effect of

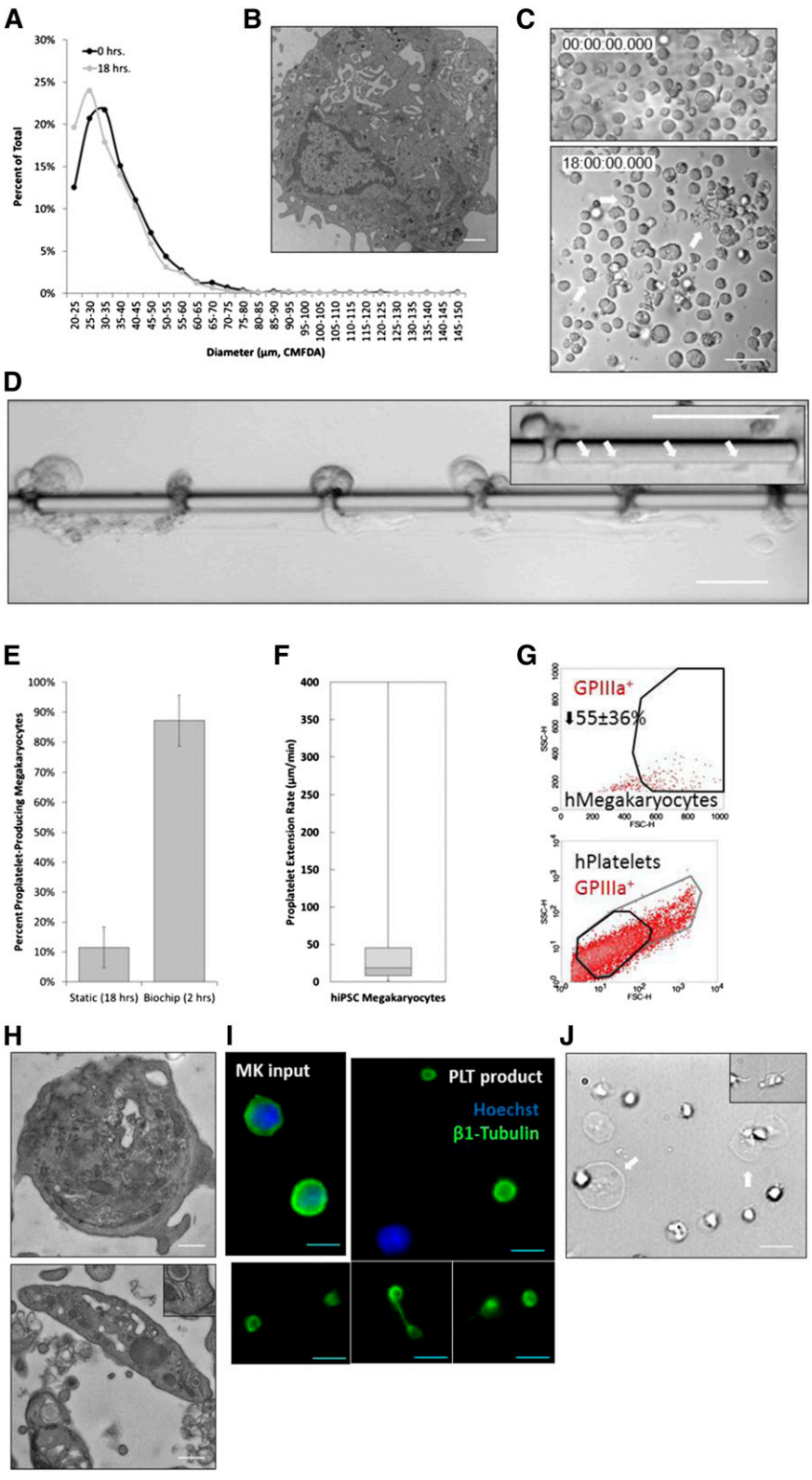

Figure 6. Bioreactor-derived hiPSC-PLTs manifest structural and functional properties of human blood PLTs. (A) The hiPSC-MKs reach maximal diameter (20-60 μm) on culture day 15. (B) The hiPSC-MKs are ultrastructurally similar to primary human MKs and contain a lobulated nuclei, invaginated membrane system, glycogen stores, organelles, and characteristic secretory granules. (C) The hiPSC-MKs in static culture begin producing proPLTs at 6 hours postpurification and reach maximal proPLT production at 18 hours. White arrows denote proPLT-producing MKs. (D) The hiPSC-MKs under physiological shear stress (~600 mPa) begin producing proPLTs immediately upon trapping and extend/release proPLTs within the first 2 hours of culture. Insert shows multiple PLT-sized swellings denoted by white arrows along single proPLT extension. (E) Percent proPLT-producing hiPSC-MKs under physiological shear stress are increased significantly to ~90% over static cultures (~10%). (F) ProPLT extension rates under physiological shear stress are ~19 μm/min. Data are represented as a box-and-whisker plot where light gray indicates the upper quartile and dark gray indicates the lower quartile. (G) Bioreactor-hPLTs display forward and side scatter, and surface biomarker expression is characteristic of human blood PLTs. (H) Bioreactor-hPLTs are ultrastructurally similar to human blood PLTs and contain a cortical MT coil, open canalicular system, dense tubular system, mitochondria, and characteristic secretory granules (both panels). Top right insert, lower panel shows peripheral MT coil. (I) Bioreactor-hPLTs are anucleate, morphologically to human blood PLTs, and display comparable MT expression. (J) Bioreactor-mPLTs form filopodia/lamellipodia on activation and are spread on a glass surface. Scale bars represent 1 μm (B), 50 μm (C-D), 0.5 μm (H), and 5 μm (I-J).

physiological stimuli on PLT formation, and PLT characterization is significantly limited.

Mounting evidence that cell-cell contacts,[22,23] ECM composition[19,20] and stiffness,[21] vascular shear stress,[24,25] pO2/pH,[51,52] soluble factor interactions,[22,53] and temperature[54] contribute to proPLT formation and PLT release have suggested that recapitulating key components of BM and blood vessel microenvironments within a three-dimensional microfluidic culture system is necessary to achieve clinically significant numbers of functional human PLTs. Our microfluidic bioreactor design expands control and resolution of the microenvironment, and has allowed us to drastically improve the time to PLT release (from 18 hours down to 2 hours) and more

than double the PLT yield. Moreover, application of vascular shear stress within our microfluidic bioreactor increased proPLT production (90% from 10%), and reproduced physiological proPLT extension and release. This study demonstrates the minimum system components required to support efficient and reproducible human platelet production in a commercial setting, and it represents the critical next step in creating an alternative source of functional human platelets for infusion.

Acknowledgments

The authors thank the staff at Advanced Cell Technologies for access to their hiPSC-derived MKs, Dr Byungwook Ahn and Dr Wilbur Lam at Emory University for their advice and support with the endothelialization of our PLT bioreactors, and Dr Markus Bender and Dr John Hartwig at Harvard Medical School for GFP-β1 tubulin viral supernatants.

This work was supported in part by grants from the Brigham Research Institute Translational Technologies and Innovation and the National Institutes of Health National Heart, Lung, and Blood Institute R01Hl68130 (J.E.I.).

J.E.I. is an American Society of Hematology Junior Faculty Scholar, J.N.T. is an American Society of Hematology Scholar, and L.M. is supported by the Marie Curie Actions – International Outgoing Fellowship (300121).

Authorship

Contribution: J.N.T. designed and performed the experiments and wrote the manuscript; J.N.T. and J.E.I. analyzed the data; L.M. and D.A.W. designed and fabricated the microfluidic bioreactors; L.M., D.A.W., and J.E.I contributed to writing the manuscript; S.W. performed many of the microfluidics, microscopy, and flow cytometry experiments; J.L.S. and K.B.N. performed the vascular shear rate modeling; A.E. performed the BM stiffness modeling; K.R.M. performed the GFP-β1 tubulin retroviral transfection; Q.F., S.L., and R.L. designed and performed the human-induced pluripotent stem cell cultures; and J.E.I. helped design the experiments.

Conflict-of-interest disclosure: Q.F., S.L., and R.L. are employees of Advanced Cell Technology, a biotechnology company in the field of stem cells and regenerative medicine. J.N.T., L.M., and J.E.I. have financial interest in and are founders of Platelet BioGenesis, a company that aims to produce donor-independent human platelets from human-induced pluripotent stem cells at scale. J.N.T., L.M., and J.E.I. are inventors on this patent. The interests of J.N.T., and J.E.I. were reviewed and are managed by the Brigham and Women's Hospital and Partners HealthCare in accordance with their conflict-of-interest policies. The interests of L.M. are managed by Harvard University in accordance with their conflict-of-interest policies. The remaining authors declare no competing financial interests.

Correspondence: Jonathan N. Thon, 1 Blackfan Circle, Karp 5, Boston, MA 02115; e-mail: drjthon@gmail.com.

References

1. Linden MD, Jackson DE. Platelets: pleiotropic roles in atherogenesis and atherothrombosis. *Int J Biochem Cell Biol.* 2010;42(11):1762-1766.
2. Battinelli EM, Markens BA, Italiano JE Jr. Release of angiogenesis regulatory proteins from platelet alpha granules: modulation of physiologic and pathologic angiogenesis. *Blood.* 2011;118(5):1359-1369.
3. Semple JW, Italiano JE Jr, Freedman J. Platelets and the immune continuum. *Nat Rev Immunol.* 2011;11(4):264-274.
4. Aster RH, Curtis BR, McFarland JG, Bougie DW. Drug-induced immune thrombocytopenia: pathogenesis, diagnosis, and management. *J Thromb Haemost.* 2009;7(6):911-918.
5. Sullivan MT, Cotten R, Read EJ, Wallace EL. Blood collection and transfusion in the United States in 2001. *Transfusion.* 2007;47(3):385-394.
6. Cobain TJ, Vamvakas EC, Wells A, Titlestad K. A survey of the demographics of blood use. *Transfus Med.* 2007;17(1):1-15.
7. Thon JN, Schubert P, Devine DV. Platelet storage lesion: a new understanding from a proteomic perspective. *Transfus Med Rev.* 2008;22(4):268-279.
8. Ohto H, Nollet KE. Overview on platelet preservation: better controls over storage lesion. *Transfus Apheresis Sci.* 2011;44(3):321-325.
9. Whitaker BI, Schlump K, Schulman J, Green J. *Report of the US Department of Health and Human Services. The 2009 national blood collection and utilization survey report.* Washington, DC: US Department of Health and Human Services, Office of the Assistant Secretary for Health; 2011.
10. Coller BS. Historical perspective and future directions in platelet research. *J Thromb Haemost.* 2011;9(Suppl 1):374-395.
11. Zhang L, Orban M, Lorenz M, et al. A novel role of sphingosine 1-phosphate receptor S1pr1 in mouse thrombopoiesis. *J Exp Med.* 2012;209(12):2165-2181.
12. Leven RM. Megakaryocyte motility and platelet formation. *Scanning Microsc.* 1987;1(4):1701-1709.
13. Leven RM, Yee MK. Megakaryocyte morphogenesis stimulated in vitro by whole and partially fractionated thrombocytopenic plasma: a model system for the study of platelet formation. *Blood.* 1987;69(4):1046-1052.
14. Tablin F, Castro M, Leven RM. Blood platelet formation in vitro. The role of the cytoskeleton in megakaryocyte fragmentation. *J Cell Sci.* 1990;97(Pt 1):59-70.
15. Junt T, Schulze H, Chen Z, et al. Dynamic visualization of thrombopoiesis within bone marrow. *Science.* 2007;317(5845):1767-1770.
16. Kaufman RM, Airo R, Pollack S, Crosby WH. Circulating megakaryocytes and platelet release in the lung. *Blood.* 1965;26(6):720-731.
17. Choi ES, Nichol JL, Hokom MM, Hornkohl AC, Hunt P. Platelets generated in vitro from proplatelet-displaying human megakaryocytes are functional. *Blood.* 1995;85(2):402-413.
18. Lambert MP, Sullivan SK, Fuentes R, French DL, Poncz M. Challenges and promises for the development of donor-independent platelet transfusions. *Blood.* 2013;121(17):3319-3324.
19. Larson MK, Watson SP. A product of their environment: do megakaryocytes rely on extracellular cues for proplatelet formation? *Platelets.* 2006;17(7):435-440.
20. Takahashi R, Sekine N, Nakatake T. Influence of monoclonal antiplatelet glycoprotein antibodies on in vitro human megakaryocyte colony formation and proplatelet formation. *Blood.* 1999;93(6):1951-1958.
21. Shin JW, Swift J, Spinler KR, Discher DE. Myosin-II inhibition and soft 2D matrix maximize multinucleation and cellular projections typical of platelet-producing megakaryocytes. *Proc Natl Acad Sci USA.* 2011;108(28):11458-11463.
22. Avecilla ST, Hattori K, Heissig B, et al. Chemokine-mediated interaction of hematopoietic progenitors with the bone marrow vascular niche is required for thrombopoiesis. *Nat Med.* 2004;10(1):64-71.
23. Fujimoto TT, Kohata S, Suzuki H, Miyazaki H, Fujimura K. Production of functional platelets by differentiated embryonic stem (ES) cells in vitro. *Blood.* 2003;102(12):4044-4051.
24. Dunois-Lardé C, Capron C, Fichelson S, Bauer T, Cramer-Bordé E, Baruch D. Exposure of human megakaryocytes to high shear rates accelerates platelet production. *Blood.* 2009;114(9):1875-1883.
25. Thon JN, Montalvo A, Patel-Hett S, et al. Cytoskeletal mechanics of proplatelet maturation and platelet release. *J Cell Biol.* 2010;191(4):861-874.
26. Thon JN, Devine MT, Jurak Begonja A, Tibbitts J, Italiano JE Jr. High-content live-cell imaging assay used to establish mechanism of trastuzumab emtansine (T-DM1)—mediated inhibition of platelet production. *Blood.* 2012;120(10):1975-1984.
27. El-Ali J, Sorger PK, Jensen KF. Cells on chips. *Nature.* 2006;442(7101):403-411.
28. Mazutis L, Gilbert J, Ung WL, Weitz DA, Griffiths AD, Heyman JA. Single-cell analysis and sorting using droplet-based microfluidics. *Nat Protoc.* 2013;8(5):870-891.
29. Prabhakarpandian B, Shen MC, Pant K, Kiani MF. Microfluidic devices for modeling cell-cell and particle-cell interactions in the microvasculature. *Microvasc Res.* 2011;82(3):210-220.
30. Kessel RG, Kardon RH. Circulating blood, blood vessels, and bone marrow. In: Johnson D, ed. *Tissues and organs: a text-atlas of scanning*

electron microscopy. San Francisco: W.H. Freeman and Company; 1979:35-50.

31. Behnke O. An electron microscope study of the rat megacaryocyte. II. Some aspects of platelet release and microtubules. *J Ultrastruct Res.* 1969; 26(1):111-129.
32. Becker RP, De Bruyn PP. The transmural passage of blood cells into myeloid sinusoids and the entry of platelets into the sinusoidal circulation; a scanning electron microscopic investigation. *Am J Anat.* 1976;145(2):183-205.
33. Winer JP, Janmey PA, McCormick ME, Funaki M. Bone marrow-derived human mesenchymal stem cells become quiescent on soft substrates but remain responsive to chemical or mechanical stimuli. *Tissue Eng Part A.* 2009; 15(1):147-154.
34. Rowley JA, Madlambayan G, Mooney DJ. Alginate hydrogels as synthetic extracellular matrix materials. *Biomaterials.* 1999;20(1):45-53.
35. Tangelder GJ, Slaaf DW, Arts T, Reneman RS. Wall shear rate in arterioles in vivo: least estimates from platelet velocity profiles. *Am J Physiol.* 1988;254(6 Pt 2):H1059-H1064.
36. Looney MR, Thornton EE, Sen D, Lamm WJ, Glenny RW, Krummel MF. Stabilized imaging of immune surveillance in the mouse lung. *Nat Methods.* 2011;8(1):91-96.
37. Mazo IB, von Andrian UH. Adhesion and homing of blood-borne cells in bone marrow microvessels. *J Leukoc Biol.* 1999;66(1):25-32.
38. Neeves KB, Onasoga AA, Wufsus AR. The use of microfluidics in hemostasis: clinical diagnostics and biomimetic models of vascular injury. *Curr Opin Hematol.* 2013;20(5):417-423.
39. Zucker-Franklin D, Philipp CS. Platelet production in the pulmonary capillary bed: new ultrastructural evidence for an old concept. *Am J Pathol.* 2000; 157(1):69-74.
40. Thon JN, Macleod H, Begonja AJ, et al. Microtubule and cortical forces determine platelet size during vascular platelet production. *Nat Commun.* 2012;3:852.
41. Patel SR, Hartwig JH, Italiano JE Jr. The biogenesis of platelets from megakaryocyte proplatelets. *J Clin Invest.* 2005;115(12): 3348-3354.
42. Fuentes R, Wang Y, Hirsch J, et al. Infusion of mature megakaryocytes into mice yields functional platelets. *J Clin Invest.* 2010;120(11): 3917-3922.
43. Lu SJ, Li F, Yin H, et al. Platelets generated from human embryonic stem cells are functional in vitro and in the microcirculation of living mice. *Cell Res.* 2011;21(3):530-545.
44. Takayama N, Nishikii H, Usui J, et al. Generation of functional platelets from human embryonic stem cells in vitro via ES-sacs, VEGF-promoted structures that concentrate hematopoietic progenitors. *Blood.* 2008;111(11):5298-5306.
45. Thon JN, Italiano JE. Platelets: production, morphology and ultrastructure. *Handb Exp Pharmacol.* 2012;210:3-22.
46. Gaur M, Kamata T, Wang S, Moran B, Shattil SJ, Leavitt AD. Megakaryocytes derived from human embryonic stem cells: a genetically tractable system to study megakaryocytopoiesis and integrin function. *J Thromb Haemost.* 2006;4(2): 436-442.
47. Takahashi K, Tanabe K, Ohnuki M, et al. Induction of pluripotent stem cells from adult human fibroblasts by defined factors. *Cell.* 2007; 131(5):861-872.
48. Nakamura S, Takayama N, Hirata S, et al. Expandable megakaryocyte cell lines enable clinically applicable generation of platelets from human induced pluripotent stem cells. *Cell Stem Cell.* 2014;14(4):535-548.
49. Ahmed RP, Ashraf M, Buccini S, Shujia J, Haider HK. Cardiac tumorigenic potential of induced pluripotent stem cells in an immunocompetent host with myocardial infarction. *Regen Med.* 2011; 6(2):171-178.
50. Nakagawa Y, Nakamura S, Nakajima M, et al. Two differential flows in a bioreactor promoted platelet generation from human pluripotent stem cell-derived megakaryocytes. *Exp Hematol.* 2013; 41(8):742-748.
51. Panuganti S, Papoutsakis ET, Miller WM. Bone marrow niche-inspired, multiphase expansion of megakaryocytic progenitors with high polyploidization potential. *Cytotherapy.* 2010; 12(6):767-782.
52. Lasky LC, Sullenbarger B. Manipulation of oxygenation and flow-induced shear stress can increase the in vitro yield of platelets from cord blood. *Tissue Eng Part C Methods.* 2011;17(11): 1081-1088.
53. Masuda S, Li M, Izpisua Belmonte JC. In vitro generation of platelets through direct conversion: first report in My Knowledge (iMK). *Cell Res.* 2013;23(2):176-178.
54. Pineault N, Boucher JF, Cayer MP, et al. Characterization of the effects and potential mechanisms leading to increased megakaryocytic differentiation under mild hyperthermia. *Stem Cells Dev.* 2008;17(3):483-493.